Chemical Geology 410 (2015) 201–212

Contents lists available at ScienceDirect

Chemical Geology

journal homepage: www.elsevier.com/locate/chemgeo

Chemical weathering controls on variations in the molybdenum isotopic composition of river water: Evidence from large rivers in China

Zhibing Wang [a,b], Jinlong Ma [a,*], Jie Li [a], Gangjian Wei [a,*], Xuefei Chen [a], Wenfeng Deng [a], Luhua Xie [c], Weijian Lu [d], Liang Zou [e]

[a] State Key Laboratory of Isotope Geochemistry, Guangzhou Institute of Geochemistry, Chinese Academy of Sciences, Guangzhou 510640, China
[b] The University of Chinese Academy of Sciences, Beijing 100039, China
[c] CAS Key Laboratory of Marginal Sea Geology, Guangzhou Institute of Geochemistry, Chinese Academy of Sciences, Guangzhou 510640, China
[d] The Fourth Middle School of Guiping, Guangxi, Guiping 537200, China
[e] Qingdao Institute of Marine Geology, Qingdao 266071, China

ARTICLE INFO

Article history:
Received 17 February 2015
Received in revised form 11 June 2015
Accepted 23 June 2015
Available online 26 June 2015

Keywords:
River water
Suspended particulates
Molybdenum isotopes
Xijiang River
Huanghe River
Chemical weathering

ABSTRACT

Mo isotopic composition in large rivers is very important for understanding global Mo cycle. At present, temporal variation signatures in the $\delta^{98/95}$Mo in large rivers have not been investigated, which hinder a comprehensive understanding on the mechanism for the variations of Mo isotopic compositions in river water. In this study, we report a one-year-long time series (March 2010 to March 2011) of the $\delta^{98/95}$Mo of both the water and suspended particulates collected at Guiping, from the middle reaches of the Xijiang River (XJR), and of the water $\delta^{98/95}$Mo from the lower reaches of the Huanghe River (HHR, or Yellow River) collected at Lijin, China. The results indicate that the temporal variations in the concentration and $\delta^{98/95}$Mo of dissolved Mo in the XJR range from 4.32 to 10.5 nmol/L (mean 7.31 nmol/L) and 1.04‰ to 1.31‰ (relative to NIST 3134) (mean 1.20‰), respectively, but that the particulates have a lower $\delta^{98/95}$Mo (−0.18‰ to 0.58‰). Analysis of the suspended particulates and other chemical parameters of the river water suggests that the weathering of silicates and sulfides is the main contributor to the dissolved Mo content in the XJR. Subsequently, the highly efficient preferential trapping of lighter $\delta^{98/95}$Mo by weathering products such as clay minerals, Fe–Mn oxides, and organic materials in soils and saprolites, which are abundant in the tropical catchment, is the key to the heavy Mo isotope signatures in the XJR. Furthermore, it seems that neither Mo-scavenging by suspended particulates during riverine transportation, nor the weathering of sulfates, significantly influences the $\delta^{98/95}$Mo of the XJR water. Cross comparison among the $\delta^{98/95}$Mo in the waters of the three largest rivers in China (the Changjiang (CJR), HHR, and XJR) indicates that the HHR has the highest Mo concentrations, but the lightest $\delta^{98/95}$Mo, the XJR has the lowest Mo concentrations but the heaviest $\delta^{98/95}$Mo, and the values for the CJR are intermediate between those for the other two rivers. This supports the conclusion that the efficiency of the selective trapping of Mo by soils and saprolites is the main factor controlling $\delta^{98/95}$Mo in these large rivers. The tropical/subtropical XJR catchment experiences intense chemical weathering, the semi-arid temperate HHR catchment experiences very little, and the CJR catchment falls somewhere between the two. Such a relationship between water Mo concentrations and $\delta^{98/95}$Mo agrees with previous observations from many large rivers worldwide. It is therefore suggested that chemical weathering on continents is the key to variations in the isotopic composition of Mo in the waters of large rivers.

1. Introduction

Molybdenum (Mo) is one of the most abundant transition metals in the oceans and is very sensitive to changes in redox conditions (Collier, 1985; Colodner, 1995; Morford and Emerson, 1999). Significant isotope fractionation occurs when Mo is removed from seawater to sediments, and the extent of this fractionation during burial is largely controlled by the redox conditions. For instance, under oxic environments, large Mo isotope fractionation occurs when Mo is adsorbed into Fe–Mn oxides, whereas little or no fractionation is observed in euxinic environments where Mo is completely scavenged (Anbar, 2004; Proemse et al., 2013; Siebert et al., 2003). Consequently, based on Mo isotopic fractionation signatures and its budget of ocean, the isotopic composition of Mo in sediments, expressed as $\delta^{98/95}$Mo, and defined as $1000 \times [(^{98}Mo/^{95}Mo)_{sample} / (^{98}Mo/^{95}Mo)_{standard} - 1]$, relative to the JMC Mo standard solution lot 602332B (Anbar, 2004; Siebert et al., 2003) or the NIST SRM 3134a (Nägler et al., 2013), can be used as a paleo-redox proxy and has been widely used to demonstrate changes in redox conditions in the global ocean, such as the great oxidation events and the expansion of

* Corresponding authors.
E-mail addresses: jlma@gig.ac.cn (J. Ma), gjwei@gig.ac.cn (G. Wei).

http://dx.doi.org/10.1016/j.chemgeo.2015.06.022
0009-2541/

reducing marine conditions in a number of periods throughout Earth's history (Anbar, 2004; Anbar et al., 2007; Arnold et al., 2004; Duan et al., 2010; Gill et al., 2011; Kendall et al., 2011; Pearce et al., 2008, 2010b; Planavsky et al., 2014; Proemse et al., 2013; Siebert et al., 2005; Wen et al., 2011; Wille et al., 2007; Zhou et al., 2010). These studies, however, have tended to adopt a critical assumption when using the quantitative interpretation of the Mo isotope record in marine sedimentary deposits to reconstruct the redox conditions of ancient oceans. This assumption was that the isotopic composition of Mo ($\delta^{98/95}$Mo) of these terrestrial inputs has remained nearly constant throughout geological history and is similar to the mean value for average basalts and granites (ca. 0.0 to 0.4‰, relative to the JMC standard; Anbar, 2004; Archer and Vance, 2008; Siebert et al., 2003).

However, this assumption has been challenged by recent measurements from a number of globally significant rivers (Archer and Vance, 2008), together with some other local rivers (Neubert et al., 2011; Pearce et al., 2010a; Voegelin et al., 2012) and estuarine waters (Rahaman et al., 2014), which indicate that the isotopic ratio of Mo in river water is not identical to the average for continental rocks, but displays a range of heavy $\delta^{98/95}$Mo values, from 0.15‰ to 2.40‰, and shows large spatial variations. Various theories have been proposed regarding the processes that control the concentration of heavy $\delta^{98/95}$Mo in river water. For instance, Archer and Vance (2008) suggested that the retention of the light $\delta^{98/95}$Mo in soils during chemical weathering is a mechanism for heavy $\delta^{98/95}$Mo in river water. Neubert et al (2011), however, indicated that weathered source rocks are the main controlling factor; in particular weathering of sulfate may account for heavy $\delta^{98/95}$Mo in river water. In addition, Mo adsorption by particulate matter during transportation has also been proposed as a possible mechanism for heavy $\delta^{98/95}$Mo in river water (Archer and Vance, 2008; Pearce et al, 2010a). At present, because of this limited set of results, it is difficult to identify the main controlling factors.

In addition to such spatial variations, temporal variations of the isotopic composition of Mo in river water are also very important in understanding the mechanisms for Mo isotope fractionation in river system and constraining its Mo isotope budget to the ocean. This, however, has received less attention in previous studies. Currently available data for river water $\delta^{98/95}$Mo observed at the same location, but at different times, are scarce. The work by Archer and Vance (2008) indicates different dry and wet season $\delta^{98/95}$Mo values for the Nile River, with a gap of 0.2‰ to 0.6‰ (higher $\delta^{98/95}$Mo during dry seasons), and the $\delta^{98/95}$Mo values in the Malaval River in southern France showed a difference of about 0.6‰ in different years (Voegelin et al., 2012). However, Neubert et al. (2011) found very small seasonal differences in the river water $\delta^{98/95}$Mo of the Kleine River in Switzerland. These results point to a possible temporal variation of river water $\delta^{98/95}$Mo. However, currently available data are too limited to accurately quantify temporal variations in river water $\delta^{98/95}$Mo for global, or even local, rivers.

Within this context, we report a one-year long time series of Mo concentrations and $\delta^{98/95}$Mo of both river water and suspended particulates collected at Guiping station in the middle reaches of the Xijiang River (XJR) in southern China, and a similar time series for river water collected at Lijin station in the lower reaches of the Huanghe River (HHR) in northern China. The XJR is the main channel of the Pearl River, the second largest river in China in terms of discharge. Located in a subtropical to tropical region, the chemical weathering intensity across the XJR catchment is much higher than most of the river basins around the world (Gaillardet et al., 1999), and laterites are widely developed in this basin. The factors controlling the $\delta^{98/95}$Mo signature and its variation in the XJR will be investigated using the chemical composition of the river water and particulates. We will show that chemical weathering over the XJR basin is the key control on the $\delta^{98/95}$Mo signature of river water.

The HHR catchment is located in a semi-arid temperate region, where chemical weathering is limited (Gaillardet et al., 1999; Wang et al., 2012) compared to that in the XJR. Cross comparisons between the XJR and HHR time series, as well as previously reported results from the Changjiang River (CJR) (Archer and Vance, 2008; Neubert et al., 2011), another large river in China, will highlight the effect of chemical weathering. Our results will improve our understanding of the temporal variations of river water $\delta^{98/95}$Mo in large rivers and the associated mechanisms, and will help to better constrain the budget for the input of terrestrial Mo isotopes to the ocean.

2. Study area

2.1. Xijiang River catchment

The XJR is the main tributary of the Pearl River, the 2th largest river in China after the CJR in terms of discharge, and covers 77.8% of the drainage area and provides 63.9% of the discharge of the Pearl River (Wei et al., 2013; Zhang et al., 2007). The XJR originates in the Maxiong Mountains in Yunnan Province and passes through Guizhou, Guangxi, and Guangdong provinces before entering the South China Sea through the Pearl River Delta in Guangdong Province (Zhang et al., 2007; Fig. 1b). The XJR catchment has a typical tropical/subtropical monsoonal climate, with mean annual temperatures ranging from 14 °C to 23 °C. The annual precipitation ranges from 1000 to 2000 mm, with most of the precipitation occurring in the rainy season from April to September. In this climate zone, vegetation flourishes, with subtropical evergreen forest dominant.

The geology of the XJR basin is complex, ranging from Precambrian metamorphic rocks to Quaternary fluvial sediments. Carbonates are the dominant rock type in the XJR catchment, covering 39% of the total basin area (Pearl River Water Resources Committee, 1991), and are mainly distributed in the upper and middle reaches of the catchment (Gao et al., 2009; Han et al., 2010; Sun et al., 2010; Xu and Liu, 2007). Silicate rocks and deposits (including igneous and metamorphic rocks and siliceous sedimentary rocks and deposits) are also widely distributed across the XJR basin, and have been intensively weathered under the humid tropical/subtropical climate to form a thick layer of red weathering crust (laterite; Gao et al., 2009). Sulfide deposits, such as pyrites, can be found in Yunnan and Guizhou provinces (Dai and Chou, 2007; Ding et al., 2001; Hu et al., 1998; Li et al., 2006, 2008; Xu et al., 2013b; Zhang et al., 2002). There is no evidence of evaporites in the XJR catchment (Wei et al., 2011, 2013; Gao et al., 2009; Xu and Liu, 2007). Chemical weathering of carbonate rocks is the main contributor to the chemistry of the XJR water, although the weathering of silicate rocks also makes a significant contribution (Zhang et al., 2007).

Guiping, located in the middle reaches of the XJR (Fig. 1b), was selected for investigation in this study. The mean annual temperature and precipitation in Guiping are 22 °C and 1700 mm, respectively. The largest tributary, the Yujiang River, joins the main stream of the XJR at the city of Guiping, where a large dam has been constructed across the tributary. To diminish the impact of human activity on the study, the observation station (23°24′47.12″N, 110°4′12.88″E) was located on the main channel of the XJR, before the river passes through Guiping city and before the Yujiang River joins the XJR. Seasonal changes in river flow at the observation station are significant, with the maximum generally being more than 5000 m^3/s during the rainy season.

2.2. Huanghe River catchment

The HHR is not one of the world's largest rivers in terms of its water discharge, but is the largest or second river in the world in terms of suspended sediment load, even though it has only a medium sized catchment (Zhang et al., 1995). Its catchment is located in the arid–semiarid climate zone of northern China (Fig. 1a), where annual precipitation ranges from 500 to 600 mm, which is less than half of the annual evaporation (Wang et al., 2012; Yang et al., 2004; Zhang et al., 1995; Zhou et al., 2014). Lijin Hydrographic Station was selected for investigation

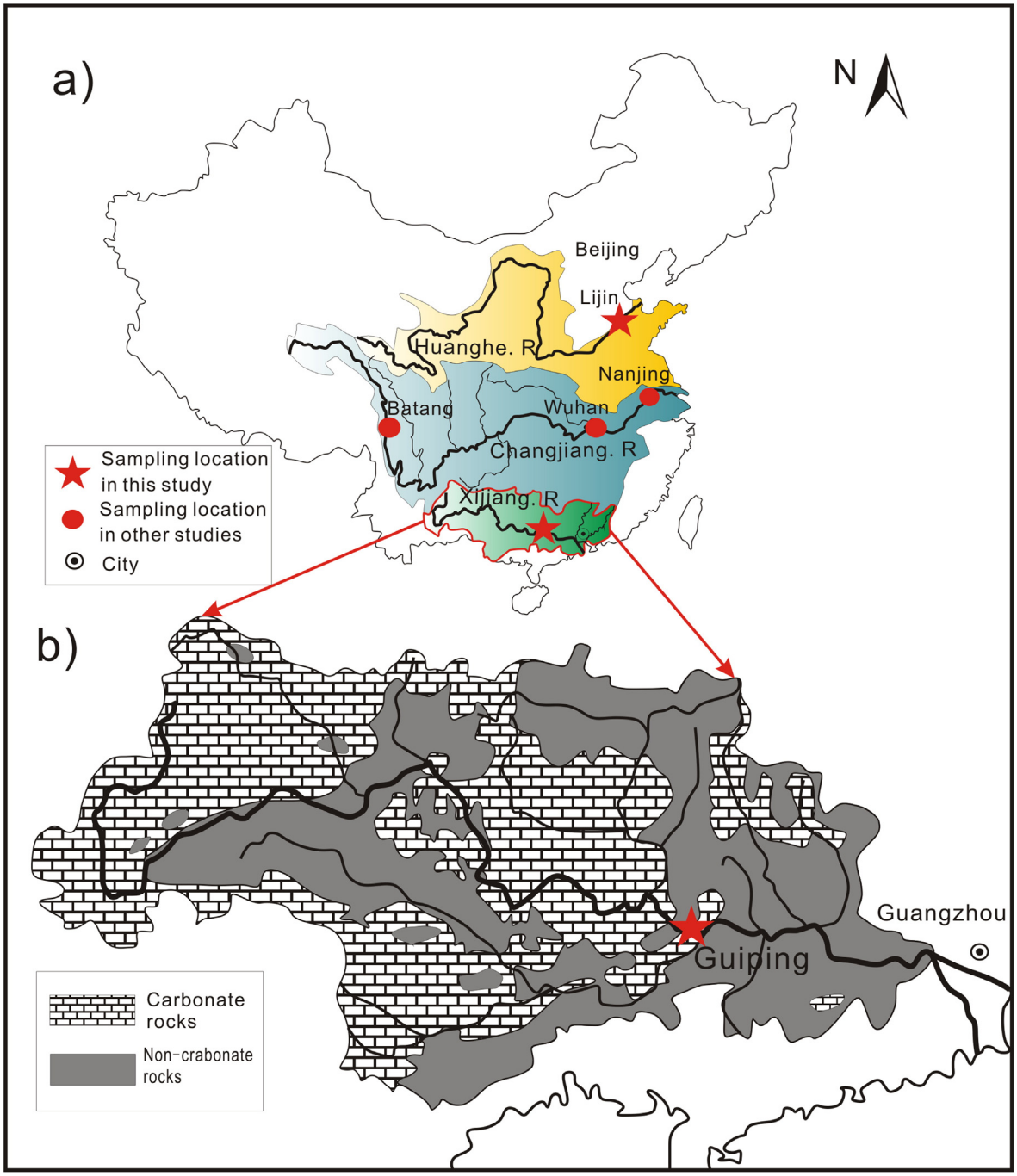

Fig. 1. a) Map showing the three major river catchments (the Huanghe, Changjiang, and Xijiang) in China and the two stations used for the time series observations at Lijin and Guiping. The locations used by Archer and Vance (2008) and Neubert et al (2011) are also shown. b) Lithological map of the Xijiang river basin adapted from Gao et al. (2009).

during this study, as it is located about 110 km upstream from the mouth of the Huanghe and is free of tidal influence (Fig. 1a).

2.3. Changjiang River catchment

The CJR is the largest river in China and the 4th largest in the world in terms of discharge, with a length of 6300 km and a drainage basin area of 1.94×10^6 km^2 (Chen et al., 2001; Yang et al., 2006; Fig. 1a). The CJR catchment is situated in a subtropical monsoon climate region where annual precipitation ranges from 600 to 900 mm (Luo et al., 2014; Xu et al., 2010; Yang et al., 2004; Zhou et al., 2014). No new sampling of the CJR was carried out as part of this study, and the Mo isotopic compositions used in the following discussion were all obtained from previous researches (Archer and Vance, 2008; Neubert et al., 2011).

3. Materials and methods

Samples for Mo isotope analysis were collected each month at Guiping, on the XJR, between March 2010 and March 2011. Temperature, pH, and conductivity were measured in the field using a Thermo Orion 4-star Plus pH/conductivity meter. River water was collected in 10 L pre-cleaned brown glass bottles from about 0.5 m below the surface in the central channel of the river. The river water was filtered through 0.45 μm Millipore membrane filters once returned to the laboratory, and both water and particulate matter samples were retained for

the following analysis. Water samples for cations, trace elements, and Mo isotope measurements were acidified immediately to pH < 2 using distilled nitric acid and then stored in polyethylene plastic (PP) bottles, whereas samples for anion analysis were directly sealed in PP bottles without acid treatment. Particulate samples were kept in cold storage at 4 °C prior to the Mo isotope measurements.

The water samples from the HHR were collected at Lijin station in the lower reaches (37°29′0.70″N, 118°15′55.18″E) between September 2012 and December 2013 at around monthly intervals by Dr. Zou Liang of the Qingdao Institute of Marine Geology. As with the XJR samples, the river water was filtered through 0.45 μm Millipore membrane filters once returned to the laboratory, acidified with distilled nitric acid, and stored in PP bottles. Water samples for cation and Mo isotope measurements were acidified immediately to pH < 2 using distilled nitric acid and then stored in PP bottles, whereas samples for anion analysis were directly sealed in PP bottles without acid treatment. Unfortunately, no field measurements were made of temperature, pH, or conductivity. Thus, detailed discussions based on these samples are difficult, and only the Mo concentrations, Mo isotopic compositions, and ion content of these samples are available for comparison with those from the XJR.

The anions and cations from the XJR and HHR water were analyzed using a Dionex ICS-900 ion chromatograph and a Thermo Element II inductively coupled plasma-atomic emission spectrometer (ICP-AES), respectively. The precision of the anion and cation measurements was generally better than 5% (RSD: relative standard deviation). The results are shown in Table 1. For details of the measurements refer to Wei et al. (2011).

The suspended particulate matter (SPM) in the XJR samples was removed and collected from the membrane filter using the following method modified from Ding et al (2011). First, the membrane filters were torn into small pieces using plastic tweezers and then immersed in deionized water in a cleaned beaker. Then, the samples were ultrasonically vibrated for 1–2 h and rinsed with deionized water for 3–5 times. Finally, the SPM were collected by centrifuging, dried at 105 °C, and weighed. The weights of the SPM samples are shown in Table 2. Trace elements concentrations (e.g., Ti) within the SPM were measured after digestion in an HF + HNO_3 mixture using a Thermo Element II inductively coupled plasma-mass spectrometer (ICP-MS). The precision of the trace element analysis was better than 3% (RSD).

The Mo isotope composition of the water and particulate samples from the XJR and the water samples from the HHR was measured using the double spike method of Li et al. (2014). The filtered and acidified water samples were spiked with a ^{100}Mo–^{97}Mo double spike solution, and allowed to equilibrate before processing for Mo separation. In the case of the particulate samples, 20–100 mg of each sample was precisely weighed and put into an individual 15 ml perfluoroalkoxy alkane beaker. A ^{97}Mo–^{100}Mo double spike solution was added to the samples, which were then well mixed. About 6 mL of a 2:1 mixture of HF (22 mol L^{-1}) and HNO_3 (14 mol L^{-1}) was then added to the samples, and the beakers were tightly capped and heated overnight on a hotplate at 120 °C. The beakers were then opened and dried at 120 °C. The samples were re-dissolved in 1 mL of concentrated HCl and dried by evaporation. Finally, the residues were re-dissolved in 2 mL of a mixture of 0.1 mol L^{-1} HF and 1 mol L^{-1} HCl, and the samples were then ready for column separation.

Molybdenum was separated and purified from the solution following the protocol given by Li et al. (2014) using a self-made extraction chromatographic resin of N-benzoyl-N-phenyl hydroxylamine. After

Table 1
Major ions and main hydrological parameters of the Xijiang River water at Guiping and the Huanghe River at Lijin station.

Sample ID[a]	Decimal year	pH[b]	T (°C)	TDS (mg/L)	Discharge[c] (m^3/s)	F^- (μmol/L)	Cl^- (μmol/L)	NO_3^- (μmol/L)	SO_4^{2-} (μmol/L)	Na^+ (μmol/L)	Mg^{2+} (μmol/L)	K^+ (μmol/L)	Ca^{2+} (μmol/L)
Xijiang River													
GPR20100320	2010.22	8.295	18.3	158	168	7.38	126	123	379	179	341	46.9	1303
GPR20100417	2010.29	8.047	18.2	146	226	7.49	179	190	389	258	332	43.8	1222
GPR20100515	2010.37	8.176	22.3	145	860	7.12	123	127	365	177	316	39.8	1241
GPR20100619	2010.47	7.808	23.3	95	14700	3.76	91	110	165	83	157	29.4	816
GPR20100717	2010.54	8.142	27.0	124	960	4.86	72	106	235	106	214	24.7	1138
GPR20100807	2010.60	7.987	26.0	131	1450	3.80	67	113	292	85	211	28.1	1202
GPR20100814	2010.62	8.078	27.1	129	820	3.67	67	115	260	94	209	26.5	1170
GPR20100920	2010.72	8.155	29.2	132	380	7.88	101	125	286	151	264	35.5	1142
GPR20100926	2010.74	7.967	27.1	133	1450	7.04	98	118	271	135	253	36.4	1205
GPR20101016	2010.79	8.101	24.7	145	390	7.23	80	138	304	139	286	36.0	1308
GPR20101121	2010.89	8.065	19.0	151	210	7.03	82	136	351	148	297	34.2	1315
GPR20101218	2010.96	8.067	17.0	135	860	7.05	104	126	302	175	275	35.8	1123
GPR20110115	2011.04	8.032	14.1	161	270	7.68	90	140	378	181	321	42.5	1353
GPR20110131	2011.08	8.117	12.1	150	236	7.67	96	144	379	193	333	42.2	1347
GPR20110215	2011.13	8.317	13.5	165	265	7.55	100	142	373	179	335	43.1	1350
GPR20110220	2011.14	8.022	13.5	153	265	11.2	104	131	353	180	324	39.3	1308
GPR20110319	2011.21	7.963	14.3	144	560	7.82	101	137	311	208	311	46.9	1190
Huanghe River													
HHR20120927	2012.74	–	–	–	1586	26.4	1671	204	1141	2967	1029	142	1169
HHR20121026	2012.82	–	–	–	381	28.8	2019	205	1241	3343	1115	140	1055
HHR20121125	2012.89	–	–	–	799	21.0	2143	169	1262	3438	1141	129	873
HHR20121225	2012.98	–	–	–	413	20.8	2336	228	1332	3662	1188	131	932
HHR20130127	2013.07	–	–	–	477	24.5	2451	248	1344	3709	1162	134	1004
HHR20130225	2013.15	–	–	–	716	23.4	3404	308	1730	4951	1383	173	1078
HHR20130324	2013.22	–	–	–	244	24.1	3236	304	1731	4990	1392	176	1488
HHR20130421	2013.30	–	–	–	204	21.7	3108	272	1675	4635	1282	166	1165
HHR20130518	2013.38	–	–	–	278	21.2	2956	258	1574	4387	1239	166	1254
HHR20130615	2013.45	–	–	–	1130	28.8	3114	203	1625	4517	1209	168	973
HHR20130716	2013.54	–	–	–	840	29.5	2599	151	1429	3958	1030	155	890
HHR20130817	2013.62	–	–	–	1580	34.5	2333	170	1384	3579	996	157	727
HHR20130916	2013.71	–	–	–	313	38.2	3003	209	1600	4346	1101	165	1190
HHR20131015	2013.79	–	–	–	218	27.5	2750	196	1483	4268	1123	149	1064

"–" indicates that the data were not measured in the field.
[a] The number in the sample ID indicates the date of sampling. For example GPR20100320 indicates that the sample was collected on March 20, 2010.
[b] The errors for the pH are generally from 0.002 to 0.003.
[c] The discharge was recorded from the web of the instant hydrological information for the main rivers in China (http://xxfb.hydroinfo.gov.cn).

Table 2
Mo concentrations and $\delta^{98/95}$Mo in water and particulate in Xijiang River.

Sample ID	Water			Particle					
	$\delta^{98/95}$Mo[a] (‰)	2SEM[b]	Mo (nmol/L)	Weight (g)	Mo (μg/g)	Ti (μg/g)	$\delta^{98/95}$Mo[a] (‰)	2SEM[b]	Ratio[c] (%)
GPR20100320	1.09	0.08	9.31	0.0202	0.96	2950	0.29	0.09	0.08
GPR20100417	1.04	0.07	10.45	0.0207	3.68	4327	0.29	0.08	0.58
GPR20100515	1.18	0.07	7.95	0.0885	2.92	5631	0.04	0.07	2.02
GPR20100619	1.30	0.11	4.32	0.2936	2.32	4617	0.02	0.05	8.51
GPR20100717	1.31	0.10	5.59	0.0778	1.93	5065	0.16	0.07	1.28
GPR20100807	1.25	0.09	5.53	0.2741	1.81	4623	0.20	0.11	4.18
GPR20100814	1.24	0.09	5.28	0.0515	3.03	4844	0.03	0.06	2.03
GPR20100920	1.18	0.08	7.79	0.0201	1.45	3257	−0.06	0.12	0.21
GPR20100926	1.17	0.10	7.55	0.3197	1.78	5833	0.05	0.11	2.52
GPR20101016	1.24	0.07	6.80	0.0556	2.41	4633	0.13	0.07	1.24
GPR20101121	1.27	0.08	7.37	0.0495	1.64	6844	0.37	0.07	0.19
GPR20101218	1.14	0.10	7.49	0.1259	1.79	5240	0.07	0.10	1.26
GPR20110115	1.14	0.08	7.33	0.0249	1.68	4637	0.58	0.18	0.27
GPR20110131	1.16	0.10	7.36	0.0361	2.23	4355	0.08	0.14	0.69
GPR20110215	1.24	0.09	7.50	0.0151	2.21	3389	−0.15	0.10	0.32
GPR20110220	1.17	0.10	7.30	0.0249	2.18	4414	0.10	0.14	0.46
GPR20110319	1.22	0.10	6.98	0.0474	3.65	5016	0.18	0.11	1.82

[a] The $\delta^{98/95}$Mo values have been calculated relative to NIST 3134.
[b] The errors are two standard deviations of the mean (2SEM).
[c] Ratio indicates the ratio of the authigenic Mo in the suspended particles to the whole Mo of the 10 L sampling river (including water and particle) in which the particles were filtered.

the separation and purification of Mo from the samples, Mo isotopic ratios were determined with a Thermo-Fisher Scientific Neptune Plus multiple collector inductively coupled plasma mass spectrometry (MC-ICP-MS). The isotopic composition of Mo was expressed as $\delta^{98/95}$Mo relative to the NIST SRM 3134 standard.

The double spike and the normalizing standard (NIST 3134) were calibrated following the procedure given by Siebert et al. (2001). The precision (two standard deviations, 2 SD) of these measurements was generally less than 0.1‰. The NIST SRM 3134 standard solution and two standard materials, IAPSO seawater and BHVO-2 basalt, were repeatedly measured along with the samples. The $\delta^{98/95}$Mo values of these standards were 0.00 ± 0.06‰ (2 SD, N = 20) for NIST SRM 3134, 2.06 ± 0.10‰ (2 SD, N = 3) for IAPSO, and 0.04 ± 0.05‰ (2 SD, N = 3) for BHVO-2, respectively. These results are consistent with certified values and the values previously reported by Greber et al. (2012) and Pearce et al. (2009), and were within analytical errors. The procedure blank for this analysis contained less than 0.06 ng of Mo, far less than the total Mo in the samples. Considering that the NIST SRM 3134 has been proposed as an international standard (Nägler et al., 2013) and its $\delta^{98/95}$Mo value is 0.25‰ greater than that of the previously used standard, the Johnson–Matthey Specpure Mo plasma standard solution (Greber et al., 2012; Li et al., 2014), the previously published data were subtracted by 0.25‰ to express them relative to the NIST 3134 standard for comparison with our $\delta^{98/95}$Mo results in the following sections.

All of the above chemical treatments and measurements were carried out in the State Key Laboratory of Isotope Geochemistry, Guangzhou Institute of Geochemistry, Chinese Academy of Science, Guangzhou, China.

4. Results

The anion and cation concentrations, as well as the other chemical properties of the river water from Guiping station on the XJR are shown in Table 1. The large seasonal variations are reflected by the marked seasonal difference in discharge, from 168 m^3/s in March 2010 to 14700 m^3/s in June 2010. Total dissolved solids (TDSs) in the river water varied from 95 to 165 mg/L, while the pH varied from 7.81 to 8.32, with low values generally corresponding to high discharge during flood events. The most abundant cation in the river water was Ca^{2+}, accounting for over 75% of the total cations, with concentrations ranging from 816 to 1353 μmol/L. The second most abundant cation was Mg^{2+}, with concentrations ranging from 157 to 341 μmol/L. The concentrations of Na^+ and K^+ ranged from 83 to 258 μmol/L and from 25 to 57 μmol/L, respectively. The concentration of SO_4^{2-} ranged from 165 to 389 μmol/L, while the concentrations of Cl^- and NO_3^- ranged from 67 to 179 μmol/L and from 106 to 190 μmol/L, respectively.

The anion and cation concentrations of the river water at Lijin station on the HHR were much larger than those from the XJR. The most abundant cation and anion were Na^+ (1670–3404 μmol/L) and Cl^- (2967–4990 μmol/L), respectively. This may explain the serious salinization of the soils in the lower reaches of the HHR. The concentrations of Mg^+, K^+, and SO_4^{2-} ranged from 996 to 1329, 129 to 176, and 1141 to 1741 μmol/L, respectively, which are 3–5 times those of the XJR. The NO_3^- concentration ranged from 151 to 308 μmol/L, about double that of the XJR, while the Ca^{2+} concentration of 727 to 1488 μmol/L was slightly less than that of the XJR.

The dissolved and particulate Mo concentrations and isotope compositions from March 2010 through March 2011 in the XJR are given, along with other parameters, in Table 2. The Mo concentration of the river water varies between 4.32 and 10.5 nmol/L, with an average of 7.17 ± 1.45 (1 SD) nmol/L, and the $\delta^{98/95}$Mo values vary between 1.04‰ and 1.31‰, with an average of 1.20 ± 0.07‰ (1 SD). These $\delta^{98/95}$Mo values are within the range reported for global rivers (Archer and Vance, 2008; Neubert et al., 2011; Pearce et al., 2010a; Rahaman et al., 2014; Voegelin et al., 2012), but heavier than that of the juvenile crustal igneous rocks (Pearce et al., 2009; Siebert et al., 2003). The Mo concentrations and $\delta^{98/95}$Mo values of the particulates ranged from 0.96 to 3.68 μg/g and −0.15‰ to 0.58‰, with a mean of 2.22 ± 0.74 μg/g (1 SD) and 0.14 ± 0.17‰ (1 SD), respectively. Similarly, the $\delta^{98/95}$Mo values of the particulates were heavier than those of juvenile crustal igneous rocks (Pearce et al., 2009; Siebert et al., 2003).

Seasonal variations of the Mo concentrations and $\delta^{98/95}$Mo values of the XJR river water can be identified clearly even though the range for $\delta^{98/95}$Mo values is very small. As shown in Fig. 2a, the Mo concentrations of the XJR river water increased from March to May, but decreased abruptly in June in 2010. From July to September, it gradually increased again. After that, Mo concentrations remained at an almost constant level. This pattern is roughly the inverse of that for discharge, which agrees with the findings of Shiller (1997), and suggests that Mo concentrations are significantly influenced by dilution by precipitation. The

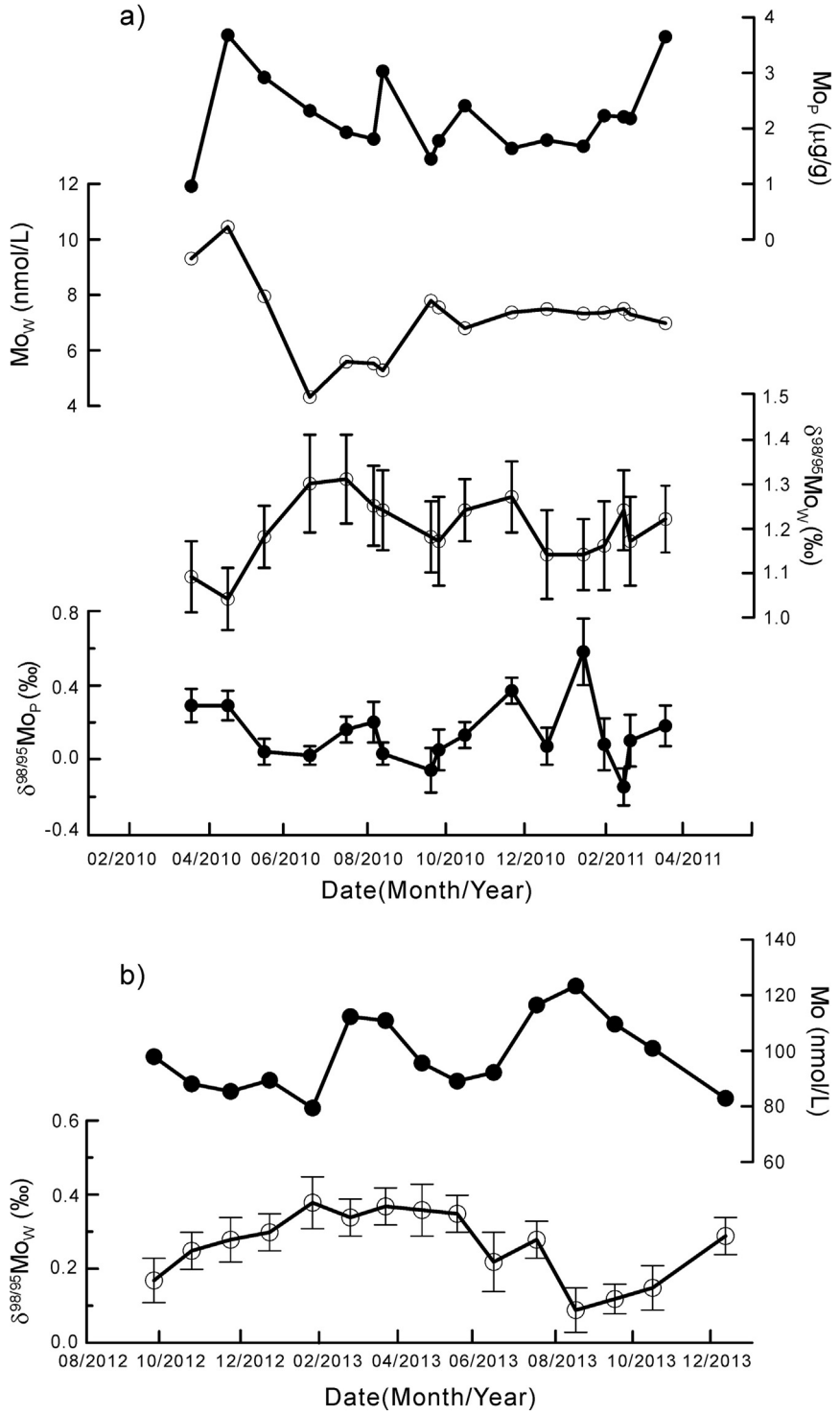

Fig. 2. Temporal variations of the Mo concentration and $\delta^{98/95}$Mo in water from the XJR and HHR. a) Time series of both the water and particulates of the XJR from March 2010 to March 2011 at Guiping station. b) Time series for the water of the HHR from September 2012 to December 2013 at Lijin station. W and P indicate water and particulate, respectively.

seasonal variation of $\delta^{98/95}$Mo is the opposite of that of the Mo concentration. In 2010, the $\delta^{98/95}$Mo in the XJR water decreased from March to May, but then increased abruptly in June. It then continued to increase gradually from July to September, and from then on remained nearly constant.

The Mo concentrations and $\delta^{98/95}$Mo found in the water from the HHR are listed in Table 3 and shown in Fig. 2b. The Mo concentrations range from 79.4 to 123.3 nmol/L, with an average of 98.2 ± 12.9 (1 SD) nmol/L, and the $\delta^{98/95}$Mo values range from 0.09 to 0.38‰, with an average of 0.26 ± 0.09‰ (1 SD). The Mo concentrations are much larger than those found in the XJR river water, but the $\delta^{98/95}$Mo values are much smaller. Nevertheless, they all are within the range reported from other global rivers (Archer and Vance, 2008; Neubert et al., 2011; Pearce et al., 2010a; Rahaman et al., 2014; Voegelin et al., 2012). The analysis of CJR water previously reported by Archer and Vance (2008) and Neubert et al (2011) is also shown in Table 3 for comparison

Table 3
Mo concentrations and $\delta^{98/95}$Mo of the water in Huanghe and Changjiang Rivers.

Sample ID[a]	$\delta^{98/95}$Mo[b] (‰)	Mo (nmol/L)	Locations	Reference
Huanghe River				
HHR20120927	0.17 ± 0.06	97.9	Lijin	This study
HHR20121026	0.25 ± 0.05	88.1	Lijin	This study
HHR20121125	0.28 ± 0.06	85.4	Lijin	This study
HHR20121225	0.30 ± 0.05	89.4	Lijin	This study
HHR20130127	0.38 ± 0.07	79.4	Lijin	This study
HHR20130225	0.24 ± 0.05	112	Lijin	This study
HHR20130324	0.37 ± 0.05	111	Lijin	This study
HHR20130421	0.36 ± 0.07	95.6	Lijin	This study
HHR20130518	0.35 ± 0.05	89.1	Lijin	This study
HHR20130615	0.22 ± 0.08	92.2	Lijin	This study
HHR20130716	0.28 ± 0.05	117	Lijin	This study
HHR20130817	0.09 ± 0.06	123	Lijin	This study
HHR20130916	0.12 ± 0.04	110	Lijin	This study
HHR20131015	0.15 ± 0.06	101	Lijin	This study
HHR20131210	0.29 ± 0.05	82.9	Lijin	This study
Changjiang River				
CJ-1	0.70 ± 0.11	16.7	Wuhan	Archer and Vance (2008)
CJ-2	0.40 ± 0.11	16.8	Wuhan	Archer and Vance (2008)
CJ-3	0.64 ± 0.11	17.1	Wuhan	Archer and Vance (2008)
CJ-4	0.58 ± 0.11	17.1	Wuhan	Archer and Vance (2008)
CJ-5	0.65 ± 0.11	15.9	Wuhan	Archer and Vance (2008)
Jin-1	0.97 ± 0.03	9	Batang	Neubert et al. (2011)
YCh3	0.86 ± 0.11	13	Nanjing	Neubert et al. (2011)

[a] The number in the sample ID of the Huanghe River indicates the date of sampling. For example HHR20120927 indicates that the sample was collected on September 27, 2012.
[b] The $\delta^{98/95}$Mo values are relative to NIST 3134, and the results from Changjiang River have been subtracted by 0.25‰ to express relative to NIST 3134. The errors are two standard deviations of the mean (2SEM).

(relative to NIST SRM 3134). The $\delta^{98/95}$Mo values of the CJR water range from 0.40‰ to 0.97‰; i.e., intermediate between those of the XJR and HHR.

5. Discussion

5.1. Sources of dissolved Mo in the Xijiang river water

Generally, dissolved Mo in river water is mainly derived from the chemical weathering of the rocks and minerals exposed in the drainage basins (Elbaz-Poulichet et al., 1999; Kaasalainen and Stefánsson, 2012; Neubert et al., 2011; Pearce et al., 2010a; Rahaman et al., 2014; Voegelin et al., 2012). The XJR catchment contains various rock types and mineral deposits, such as carbonates, silicate rocks, and sulfate and sulfide minerals, but carbonates and silicates are the dominant lithology of the XJR catchment (Pearl River Water Resources Committee, 1991). Carbonates, mainly limestone, dominate the drainage basin, in particular in the upper and middle reaches of the XJR (Gao et al., 2009).

The source of the dissolved Mo can be inferred by comparing the Mo concentrations to the chemical compositions of the river water. As Ca^{2+} in river water is mainly derived from the weathering of carbonates, and K^+ mainly from the weathering of silicates (Gaillardet et al., 1999), we used the Ca^{2+} and K^+ concentrations to indicate the contribution from the weathering of carbonates and silicates, respectively. Even though anthropogenic sulfuric acid contributes significantly to the SO_4^{2-} levels in the river water in the upper reaches of the XJR, particularly in the regions around the large cities of Guizhou Province where acid precipitation is a serious issue because of the heavy coal consumption (Li et al., 2008; Xu and Liu, 2007), the majority of the river water SO_4^{2-} is still derived from the oxidative weathering of sulfide minerals (Li et al., 2008), and this contribution could be larger across the whole of the XJR basin. Consequently, we used the SO_4^{2-} levels of the river water to indicate the contribution from weathering of sulfide/sulfate minerals. The discharge of the XJR shows very large seasonal variations (Wei et al., 2013), and the concentrations of Mo and the other major ions in the XJR water are significantly diluted during the rainy season. To reduce the impact of this dilution effect, we normalized the Mo, Ca^{2+}, K^+, and SO_4^{2-} concentrations by the total dissolved solid (TDS), and the results are shown in Fig. 3.

There is a weak negative correlation between Mo/TDS and Ca^{2+}/TDS (Fig. 3a), indicating that enhanced Ca^{2+} input to the river water from the weathering of carbonates appears to be associated with a lower Mo input. Thus, weathering of carbonates may not be the main source of dissolved Mo in the XJR water, even though outcrops of carbonaceous rocks occupy about 39% of the XJR basin (Pearl River Water Resources Committee, 1991). This is supported by research showing that Mo concentrations in carbonate rocks such as limestone are very low (<1 μg/g; Voegelin et al., 2009, 2010). Moreover, if the dissolved Mo is mainly derived from the dissolution of carbonates by chemical weathering, the Mo/Ca^{2+} ratios in the river water might be similar to that in carbonate rocks, of around 2.9×10^{-7} (Zhu and Lin, 1996; Voegelin et al.,

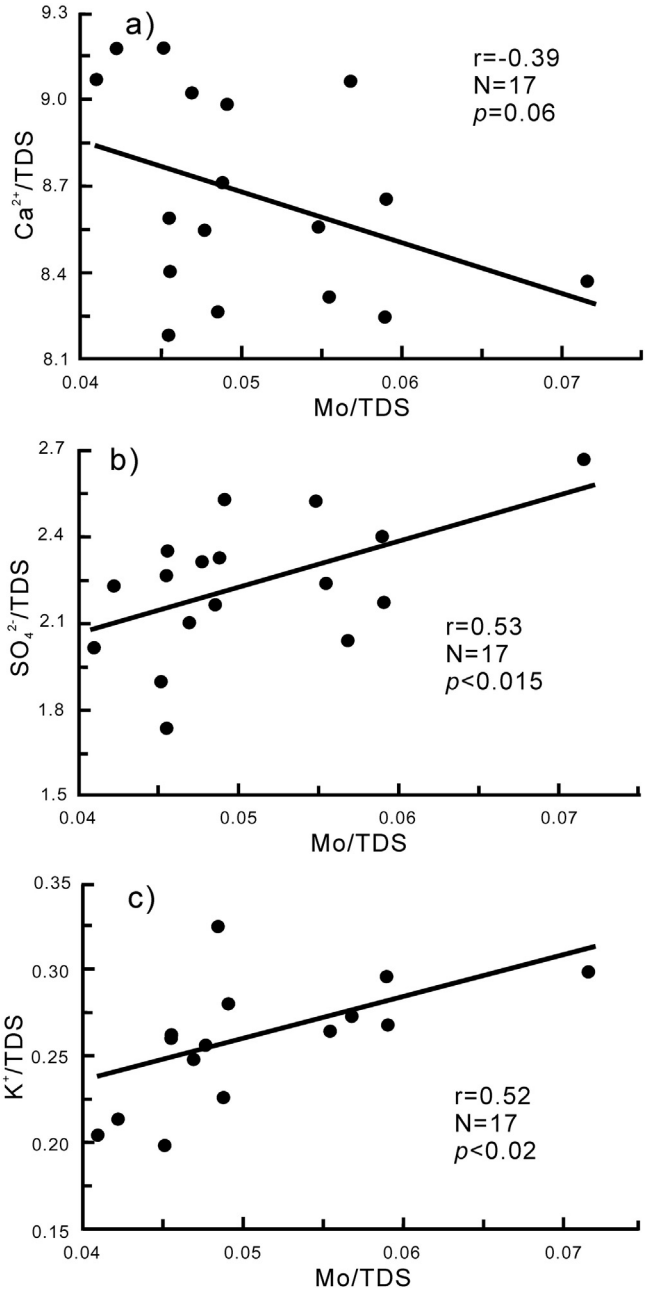

Fig. 3. Correlations between Mo/TDS and a) Ca^{2+}/TDS, b) SO_4^{2-}/TDS, and c) K^+/TDS for the XJR water.

2009). However, the Mo/Ca^{2+} ratios of the XJR water range from 4.5×10^{-6} to 8.6×10^{-6}, with an average of $5.9 \pm 1.0 \times 10^{-6}$, which is as much as twenty times higher than that in carbonate rocks. Therefore, weathering of carbonate rocks may not be the main source of the dissolved Mo in the XJR water.

Both SO_4^{2-}/TDS and K^+/TDS show statistically significant positive correlations with Mo/TDS in the XJR water (Fig. 3b and c), with correlation coefficients of 0.53 ($N = 17$, $p < 0.015$) and 0.52 ($N = 17$, $p < 0.017$), respectively. This suggests that weathering of silicate rocks and sulfate or sulfide minerals both contribute to the dissolved Mo in the XJR water. Following that of the carbonate rocks outcrops, silicate rocks are also widely distributed across the XJR catchment, and sulfide mineral deposits (such as pyrites) can generally be found in the upper reaches of the XJR, such as in Yunnan and Guizhou provinces (Dai and Chou, 2007; Ding et al., 2001; Hu et al., 1998; Li et al., 2006, 2008; Xu et al., 2013b; Zhang et al., 2002). Meanwhile, the Mo concentrations in the silicate rocks from the XJR basin are reported to be 1–5 μg/g Mo (Huang et al, 1996), and those in the sulfide minerals are higher at 10^1–10^2 μg/g (Malinovsky et al., 2005, 2007) or even up to 7×10^5 μg/g (Xu et al., 2013b). Weathering of such materials appears to be sufficient to supply the dissolved Mo found in the XJR water at concentrations of 4.3–10.5 nmol/L (Table 2). Therefore, we conclude that weathering of silicate rocks and sulfide minerals might be the main sources of the dissolved Mo in the XJR water.

5.2. Controls on the $\delta^{98/95}$Mo of the dissolved Mo in the XJR water

As shown in Fig. 2, the $\delta^{98/95}$Mo of the dissolved Mo of the XJR water during 2010–2011 ranges from 1.05‰ to 1.31‰, with a mean of 1.20 ± 0.07‰ (1 SD). These values are much heavier than those seen in the juvenile crustal igneous rocks (Pearce et al., 2009; Siebert et al., 2003), and higher than most of the previously reported river water $\delta^{98/95}$Mo values around the world (Archer and Vance, 2008; Neubert et al., 2011; Pearce et al., 2010a; Voegelin et al., 2012). Several possible processes have been proposed to account for the heavy $\delta^{98/95}$Mo values in river water. The first is removal of Mo with lower $\delta^{98/95}$Mo from river water as it is adsorbed onto the suspended particulates during transportation (Barling and Anbar, 2004; Goldberg et al., 2009; Pearce et al., 2010a). The second is fractionation during chemical weathering of rocks, by which Mo containing lighter $\delta^{98/95}$Mo tends to be retained in soils and saprolites (Ma et al., Submitted for publication; Pearce et al., 2010a; Pett-Ridge et al., 2008; Siebert et al., 2009, 2015; Voegelin et al., 2012). The third is a contribution from weathering of sulfate minerals such as gypsum (Neubert et al., 2011).

As the suspended particulates were quantitatively filtered from the 10 L water samples, the Mo concentration and $\delta^{98/95}$Mo of both the water and the SPM listed in Table 2 enable us to estimate the influence of suspended particulate adsorption on river water $\delta^{98/95}$Mo. Estimated from the major and trace elements of the SPM (unpublished data) silicate detritus compose of the main of the SPM. Given that a considerable proportion of the Mo in the particulates is derived from detrital materials, we first calculated the concentrations of the adsorbed Mo (i.e., the authigenic Mo) in the particulate matter by using the following equation and assuming that all of the Ti in the SPM is contributed from detrital materials:

$$Mo_{authigenic} = Ti_{particulate} \times \left[(Mo/Ti)_{particulate} - (Mo/Ti)_{EC}\right]$$

where $Mo_{particulate}$ and $Ti_{particulate}$ represent the Ti and Mo concentrations in the particulate matter, respectively, and $(Mo/Ti)_{EC}$ is the mean Mo/Ti ratio of the East China crust, which covers most of the XJR catchment (Gao et al, 1999). The calculated authigenic Mo concentrations in the SPM range from 0.27 to 2.81 μg/g, with a mean of 1.28 μg/g. This accounts for 34.5% to 76.5% of the total Mo in the SPM. Meanwhile, the ratio of the authigenic Mo to the total Mo in the 10 L water samples (including water and the suspended particulates), expressed as f_{AP} was calculated and is listed in Table 2. The results indicate that the authigenic Mo accounts for only a small part of the total Mo in the river water, ranging from 0.08% during the lowest discharge period (March 20, 2010) to 9.0% during flood events (June 19, 2010), and with an average of 1.7%.

We then estimated the $\delta^{98/95}$Mo of the authigenic Mo in the SPM by using the following equation:

$$\delta^{98/95}Mo_{particulate} = f_{authigenic} \times \delta^{98/95}Mo_{authigenic} + \left(1 - f_{authigenic}\right) \times \delta^{98/95}Mo_{detritus}$$

where $f_{authigenic}$ indicates the proportion of authigenic Mo in total Mo in the particulates. The $\delta^{98/95}Mo_{detritus}$ may be close to that of the continental crust, of about 0‰, relative to the JMC standard (Siebert et al., 2003). The calculated authigenic $\delta^{98/95}$Mo values are generally less than 1‰, with an average of 0.9‰.

Finally, the $\delta^{98/95}$Mo of the original water, before Mo adsorption by particulates, was calculated using the following equation:

$$\delta^{98/95}Mo_{original} = (1 - f_{AP}) \times \delta^{98/95}Mo_{water} + f_{AP} \times \delta^{98/95}Mo_{authigenic}$$

where f_{AP} and $\delta^{98/95}Mo_{authigenic}$ refer to the above calculation, and $\delta^{98/95}Mo_{water}$ is the measured value of the filtered water listed in Table 2. The calculated $\delta^{98/95}$Mo values of the original water range from 1.04‰ to 1.30‰, with an average of 1.18‰. These values are very close to those of the river water after particulate adsorption for that the ratios of the authigenic Mo in the SPM to the total Mo of the river water is very small. The estimated gaps between $\delta^{98/95}Mo_{water}$ and $\delta^{98/95}Mo_{original}$ range from 0‰ to 0.10‰, with an average of 0.014‰, which are within the range of the analytical errors. This indicates that the removal of Mo with relatively lighter $\delta^{98/95}$Mo from river water via adsorption onto particulates appears to have little effect on the $\delta^{98/95}$Mo in river water, which agrees with the findings of Archer and Vance (2008) and Pearce et al. (2010a).

This can further be supported by a comparison of the $\delta^{98/95}$Mo–[Mo] relationship in the particulate and the dissolved phases. Even though the range for the $\delta^{98/95}$Mo of the XJR water was fairly small (from 1.04‰ to 1.31‰), the inverse relationship between Mo concentrations and $\delta^{98/95}$Mo values is evident. As shown in Fig. 4a, $\delta^{98/95}$Mo shows a significant negative correlation with Mo ($r = -0.85$, $N = 17$, $p < 0.000005$) in the river water over the sampling period. Such trend can be seen in many large rivers around the world (Archer and Vance, 2008; Neubert et al., 2011). If the $\delta^{98/95}$Mo variation of the dissolved Mo is modified by adsorption of authigenic Mo in the SPM, there may be an inverse correlation between the $\delta^{98/95}$Mo and Mo concentration in the SPM for that Mo with lighter $\delta^{98/95}$Mo tends to be adsorbed by SPM during the absorption process, and the more Mo with lighter $\delta^{98/95}$Mo is adsorbed, the heavier $\delta^{98/95}$Mo retains in river water. This, however, is not observed in the XJR SPM. As shown in Fig. 4b, there is no apparent positive correlation between the $\delta^{98/95}$Mo and Mo concentrations in the SPM with a correlation of −0.13 ($N = 17$, $p = 0.31$), indicating that the particulate adsorption process takes little effect to the dissolved $\delta^{98/95}$Mo.

It is worth noting that the $\delta^{98/95}$Mo gaps between the river water and SPM, defined as $\Delta\delta^{98/95}Mo_{W-P} = \delta^{98/95}Mo_W - \delta^{98/95}Mo_P$ of the XJR are not constant through the whole year. The $\Delta\delta^{98/95}Mo_{W-P}$ values are ranging from 0.56‰ to 1.39‰, with an average of 1.06 ± 0.21‰ (1σ), which is larger than the range of the dissolved $\delta^{98/95}$Mo. There exists an apparent negative correlation between the $\Delta\delta^{98/95}Mo_{W-P}$ and concentrations of dissolved Mo ($r = -0.51$, $N = 17$, $p = 0.037$) (Fig. 4c). It is likely that the $\delta^{98/95}$Mo gap between the river water and SPM may be less when Mo concentration in river is higher. However, such large variation of $\Delta\delta^{98/95}Mo_{W-P}$ is mainly contributed from large variation of particulate $\delta^{98/95}$Mo (up to 0.7‰) rather than that of

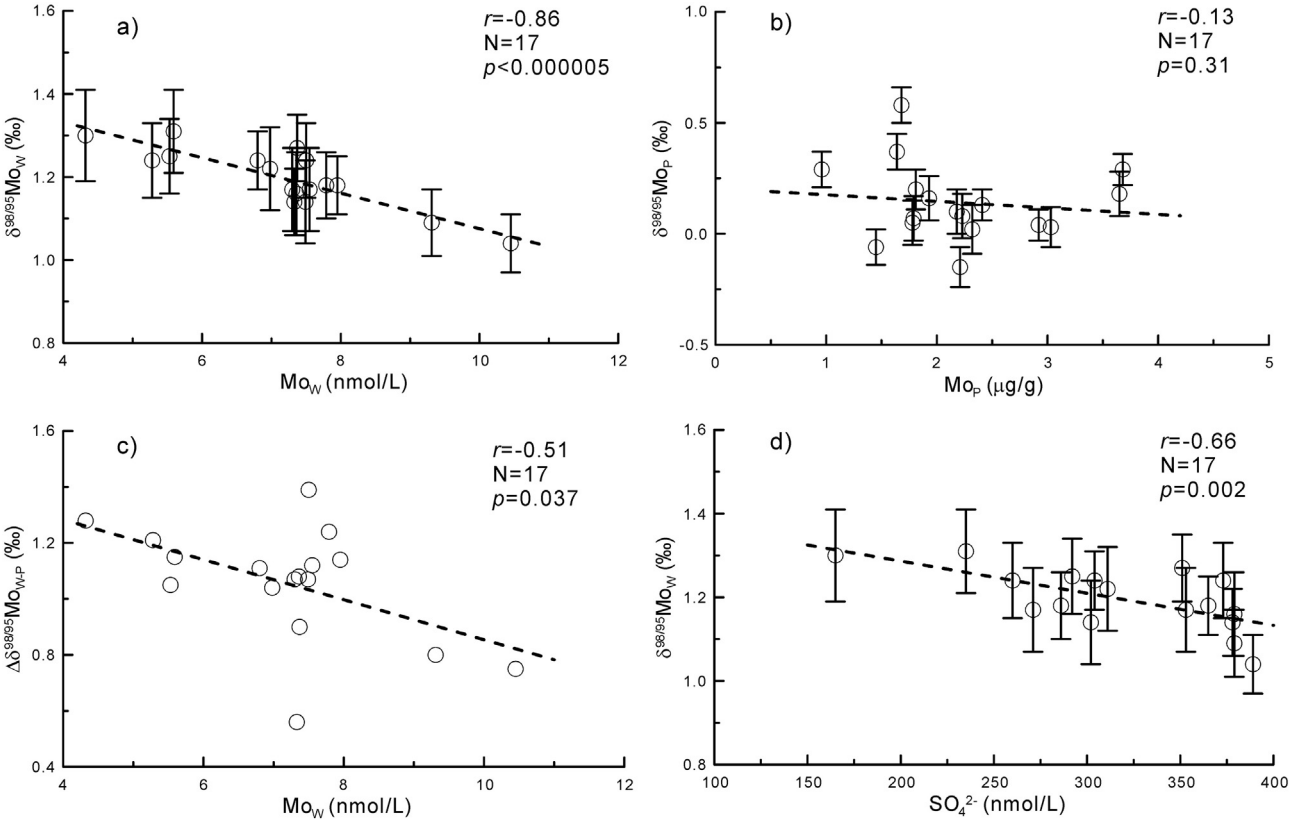

Fig. 4. a) Correlations between $\delta^{98/95}$Mo and Mo concentrations in the water; and b) in the particulates of the XJR; c) correlation between the $\delta^{98/95}$Mo gaps between the water and particulate and Mo concentrations in the water of the XJR; and d) correlation between $\delta^{98/95}$Mo and SO_4^{2-} concentrations in the XJR water. W and P indicate water and particulate, respectively.

the dissolved Mo. The apparent correlation between the $\Delta\delta^{98/95}Mo_{W-P}$ and concentrations of dissolved Mo likely indicates the influence of dissolved Mo on the $\delta^{98/95}$Mo of particulates, and in turn, the influence of authigenic Mo adsorbed by particulates to the $\delta^{98/95}$Mo of the dissolved Mo in river water is negligible. Therefore, the fairly heavy $\delta^{98/95}$Mo values of the XJR water may not be the result of modification by particulate adsorption, but are instead generated by the input of Mo with high $\delta^{98/95}$Mo derived from chemical weathering in the XJR basin.

As mentioned above, the dissolved Mo of the XJR water is mainly derived from the weathering of silicate rocks and sulfide/sulfate minerals across the basin. Weathering of sulfates, such as gypsum, in the catchment can supply dissolved Mo with a high $\delta^{98/95}$Mo, because gypsum originates from the evaporation of seawater and generally has a high $\delta^{98/95}$Mo values (Neubert et al., 2011). In this case, river water $\delta^{98/95}$Mo will show a positive correlation with SO_4^{2-} concentrations (Neubert et al., 2011). However, this is not observed in the XJR water. Currently, no large sulfate-rich evaporite deposits have been found in the XJR catchment (Pearl River Water Resources Committee, 1991). Moreover, there is a moderate negative correlation ($r = -0.66$, N = 17, $p < 0.002$), rather than a positive correlation, between $\delta^{98/95}$Mo and SO_4^{2-} concentrations in the river water (Fig. 4d). This suggests that the fairly high $\delta^{98/95}$Mo of the XJR water is not derived from the weathering of sulfates.

In addition to weathering of sulfates, oxidization of sulfides during chemical weathering may also provide SO_4^{2-} to river water. Currently available $\delta^{98/95}$Mo results of the sulfide minerals in the XJR catchment show a large variation range from 0.69‰ to 1.13‰, with a mean of 0.88 ± 0.15‰ relative to NIST 3134 (Xu et al., 2013b). These values are generally lower than those of the XJR river water (from 1.04‰ to 1.31‰ with a mean of 1.20 ± 0.07‰). Thus they may not be the contributor for the high $\delta^{98/95}$Mo of the dissolved Mo in the XJR. Considering the negative correlation between $\delta^{98/95}$Mo and SO_4^{2-} concentrations shown in Fig. 4d, enhanced input of dissolved Mo from weathering of sulfides likely decreases the $\delta^{98/95}$Mo of the river water, due to the relative lower $\delta^{98/95}$Mo of the sulfides than those of the river water. It is therefore that weathering of sulfides may not be the reason for the high $\delta^{98/95}$Mo of the XJR water either.

Significant Mo isotope fractionation has been observed during chemical weathering of silicate rocks, and such fractionation is probably associated with the pH and redox conditions in the weathering profile (Ma et al., Submitted for publication; Pearce et al., 2010a; Pett-Ridge et al., 2008; Siebert et al., 2009, 2015). During chemical weathering, Mo, together with other highly mobile elements, such as Na, Mg, and Sr, is easily removed from the parent rocks and transported into watercourses (Gaillardet et al., 2005). A considerable proportion of this removed Mo is easily trapped by organic matter, clay minerals, and Fe–Mn oxides and retained on saprolites and soils, in which organic matter is one of the most important hosts for Mo (Ma et al., Submitted for publication; Wichard et al., 2009; Xu et al., 2013a; Siebert et al., 2009, 2015).

Generally, Mo with lighter $\delta^{98/95}$Mo is preferentially adsorbed by weathering products (Pearce et al., 2010a; Pett-Ridge et al., 2008; Siebert et al., 2009, 2015), and Mo with a heavier $\delta^{98/95}$Mo is transported to streams and rivers (Archer and Vance, 2008; Neubert et al., 2011; Pearce et al., 2010a; Voegelin et al., 2012). Moreover, organic matter in saprolites and soils also preferentially traps Mo with lighter $\delta^{98/95}$Mo (Ma et al., submitted for publication; Siebert et al., 2015). Therefore, if the efficiency of the trapping of Mo by soils and saprolites is enhanced across a basin, more Mo activated during chemical weathering is trapped, and of which Mo with a lighter $\delta^{98/95}$Mo is preferentially trapped. As a result, the amount of Mo released to rivers will decrease, but its $\delta^{98/95}$Mo values will increase, and an inverse relationship will develop between Mo concentrations and $\delta^{98/95}$Mo in river

water, such as the positive correlation between $\delta^{98/95}$Mo and 1/[Mo] observed by Archer and Vance (2008) and Neubert et al. (2011).

The significant negative correlation between $\delta^{98/95}$Mo and Mo concentrations in the river water shown in Fig. 4a suggests that trapping of activated Mo during chemical weathering in soils and saprolites across the XJR catchment has a significant effect on the isotopic composition of Mo in the XJR water. This agrees with the geological background of the XJR basin. Located in a subtropical to tropical region, the intensity of chemical weathering across the XJR catchment is very high, and laterites are widely developed and support a flourishing flora. Clay minerals, Fe–Mn oxides, and organic matter are abundant in the soils and saprolites (Dai and Huang, 2006; Yu et al., 2007), and the capacity for trapping Mo is apparently large. As a result, the Mo released to rivers should be small and its $\delta^{98/95}$Mo value should be high.

In summary, the XJR water has low Mo concentrations but high $\delta^{98/95}$Mo values, which may be attributed to the high efficiency of the soils and saprolites in trapping Mo across the drainage basin. Adsorption to suspended particulates during transportation does not significantly change the river water $\delta^{98/95}$Mo, and weathering of sulfate and sulfide minerals does not contribute to the high $\delta^{98/95}$Mo values of the XJR water.

5.3. Comparisons with other rivers

The CJR, HHR, and XJR are the three largest rivers in China, but their catchments are located in different climate belts. Comparison of the river water $\delta^{98/95}$Mo among these rivers may provide an indication of the relevant controlling factors. As shown in Fig. 2b, the $\delta^{98/95}$Mo time series of the HHR water collected at Lijin shows very small variations (0.09‰ to 0.38‰, with an average of 0.26 ± 0.09‰; 1 SD), in which the standard deviation is similar to the analytical error. This is similar to that of the XJR time series established at Guiping, suggesting that seasonal variation of the $\delta^{98/95}$Mo of the water in the large rivers in China is very small. There is no river water $\delta^{98/95}$Mo time series available for the CJR, so seasonal variation in the CJR could not be evaluated here. Controlled by the East Asian monsoon, seasonal climate changes are very large across these catchments. The very small seasonal variations of the dissolved $\delta^{98/95}$Mo in both the XJR and the HHR suggest that short-term climate change has no significant influence on the isotopic composition of Mo in the river water in these catchments.

However, both the Mo concentrations and the $\delta^{98/95}$Mo values of the water in these three rivers were significantly different. The XJR had the lowest Mo concentrations and highest $\delta^{98/95}$Mo with means of 7.17 ± 1.45 nmol/L and 1.20 ± 0.07‰, respectively, whereas the HHR had the highest Mo concentrations and lowest $\delta^{98/95}$Mo with means of 98.2 ± 13.4 nmol/L and 0.26 ± 0.09‰, respectively. The results for the CJR, with means of 15.1 ± 3.0 nmol/L and 0.69 ± 0.19‰ for Mo concentration and $\delta^{98/95}$Mo, respectively, reported by Archer and Vance (2008) and Neubert et al (2011), lie between those of the XJR and HHR. It is worth noting that there is a robust negative correlation between the Mo concentrations and the $\delta^{98/95}$Mo of the water in CJR, which is similar to that of the seasonal changes in the XJR and the HHR water, and those reported by Archer and Vance (2008) and Neubert et al. (2011) expressed as $\delta^{98/95}$Mo–1/[Mo] correlation. Fig. 5a shows the correlation between $\delta^{98/95}$Mo and 1/[Mo] for the CJR, HHR, and XJR. The great correlation coefficient ($r^2 = 0.92$) was obtained from the logarithmic regression (N = 39, $p < 0.0000001$). Such a significant correlation, as well as the spatial difference of the three large rivers, suggests that the variation of these Mo isotopic compositions is driven by a similar mechanism.

As mentioned above, and according to Archer and Vance (2008), Pearce et al. (2010a), and Neubert et al. (2011), Mo adsorption to suspended particulates may not change the $\delta^{98/95}$Mo in river water significantly. This could be again inferred from the following comparison. As for these three rivers, the HHR carries one of the highest suspended sediment loads in the world (Zhang et al., 1995). Consequently, Mo

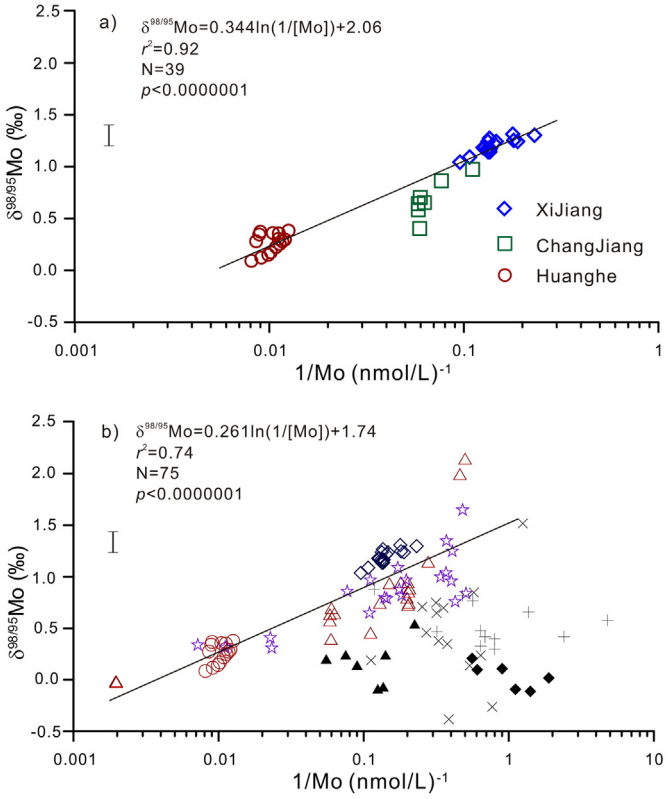

Fig. 5. a) The correlation between $\delta^{98/95}$Mo and 1/[Mo] for the HHR, CJR, and XJR water. The CJR data are from Archer and Vance (2008) and Neubert et al. (2011). b) The correlation between $\delta^{98/95}$Mo and 1/[Mo] for the CJR and HHR, and also for other world rivers from Archer and Vance (2008) and Neubert et al. (2011), marked by the open symbols. The data from the Nile (solid diamonds) reported by Archer and Vance (2008), from the Kleine Fontanne and Trueb (solid triangles) in the Entlebuch catchment in Switzerland reported by Neubert et al. (2011), from the rivers (fork) in Iceland reported by Pearce et al. (2010a), and the Malaval and Séjallières (cross) reported by Voegelin et al. (2012) are not included in the regression calculation. The error bars indicate the mean analytical error of the $\delta^{98/95}$Mo.

adsorption should be greatest in the HHR. However, the $\delta^{98/95}$Mo of the HHR water was the lowest among these three rivers, indicating that Mo adsorption may not be the reason for the observed spatial differences in $\delta^{98/95}$Mo.

Weathering of sulfate minerals may also not be an important factor for such spatial differences in $\delta^{98/95}$Mo. As shown in Table 1, the SO_4^{2-} concentrations of the HHR water are 3–5 times those of the XJR water, and the SO_4^{2-} concentrations in the CJR water of 310–970 nmol/L (Neubert et al., 2011) are generally higher than those of the XJR water of 165–379 nmol/L with a mean of 317 nmol/L, but their $\delta^{98/95}$Mo values are all lighter than those of the XJR water. This does not agree with a scenario of a significant contribution from sulfate weathering to the dissolved Mo in river water (Neubert et al., 2011).

Selective trapping of Mo activated during chemical weathering of soils and saprolites could certainly explain the spatial difference in both the Mo concentration and $\delta^{98/95}$Mo of the water among these three large rivers. The HHR river basin is located mainly in an arid–semiarid climate zone in northern China, where the annual precipitation ranges from 500 to 600 mm, which is less than half of the annual evaporation (Wang et al., 2012; Yang et al., 2004; Zhang et al., 1995; Zhou et al., 2014). However, the CJR basin experiences a subtropical monsoon climate where the annual precipitation ranges from 600 to 900 mm (Luo et al., 2014; Xu et al., 2010; Yang et al., 2004; Zhou et al., 2014). The climate of the XJR basin is typical of the tropical/subtropical monsoonal style, with mean annual temperatures ranging from 14–23 °C, and annual precipitation ranging from 1000–2000 mm (Wei et al., 2013; Xu and Han, 2009). Laterites are widely developed

across the XJR catchment, and vegetation flourishes, and these conditions provide abundant clay minerals, Fe–Mn oxides, and organic matter that favors the trapping of Mo in soils and saprolites.

In contrast, loess dominates the HHR catchment, and vegetation is sparse (Dai and Huang, 2006; Liu et al., 2011; Yu et al., 2007). The capacity for trapping Mo in soils and saprolites across the HHR catchment should therefore be small. The situation in the CJR catchment is likely to be midway between those of the XJR and HHR basins. As a result, less dissolved Mo is released to the water of the XJR than to the HHR, leading to lower Mo concentrations but heavier $\delta^{98/95}$Mo in the XJR water than in the HHR. Both the Mo concentrations and $\delta^{98/95}$Mo of the CJR water lie in between those of the XJR and HHR. It is therefore likely that the differences in soils and saprolites related to chemical weathering in the catchments may account for the spatial difference in Mo concentrations and $\delta^{98/95}$Mo among these three large rivers.

Such a negative correlation between Mo concentrations and $\delta^{98/95}$Mo in the water of the three largest rivers in China agrees with the previously reported results from other rivers around the world (Archer and Vance, 2008; Neubert et al., 2011). Fig. 5b shows data from XJR, HHR, and those reported by Archer and Vance (2008) and Neubert et al. (2011); note that the results from the CJR are from these two studies and have also been included. These data present a robust logarithmic regression ($r^2 = 0.74$, N = 75, $p < 0.0000001$) that is similar to that of the large rivers in China. This suggests that selective adsorption by soils and saprolites across the catchments may also be an important factor in controlling the dissolved Mo concentrations and isotopic compositions in many rivers around the world.

However, there are also some exceptions. The data from the Nile River reported by Archer and Vance (2008) and from the Kleine Fontanne and Trueb rivers in the Entlebuch catchment in Switzerland reported by Neubert et al. (2011), shown as solid diamonds and solid triangles, respectively in Fig. 5b, were excluded from the above regression. In addition to these two rivers, the data from two small streams in southern France (Voegelin et al., 2012) and from several streams in Iceland (Pearce et al., 2010a) do not show this correlation either. These rivers and streams generally have small catchments (e.g., those in France and Switzerland), or drain through desert (e.g., the Nile) or frozen regions (e.g., those in Iceland). The intensity of chemical weathering in these regions is apparently low, and the development of soils and saprolites is limited. Consequently, there should be little Mo activated from rocks during weathering, and isotopic fractionation of Mo caused by selective adsorption by soils and saprolites should also be weak, resulting in low Mo concentrations and $\delta^{98/95}$Mo values in the water of these streams/rivers (Fig. 5b). Given that there are numerous factors that influence the isotopic composition of Mo in river water, and that currently available data are limited, more work will be required if we are to develop a better understanding of the mechanisms that drive variations in dissolved Mo isotopes in rivers around the world.

6. Conclusions

This study analyzed a one-year-long time series of the isotopic composition of Mo in both the river water and suspended particulates from the Xijiang River, and of the river water from the Huanghe River, as well as other chemical parameters of the river water, to investigate the variations in the isotopic composition of Mo in large Chinese rivers and the associated mechanisms. Our main findings are outlined below.

1) The dissolved Mo in the XJR water is derived mainly from the weathering of silicate rocks and sulfide minerals across the XJR drainage basin, and the contribution from the weathering of carbonates is small, even though they dominate outcrops in the XJR catchment.
2) The XJR water has fairly high $\delta^{98/95}$Mo values, but seasonal variations are very small and show a robust negative correlation with the Mo concentrations. Preferential trapping of Mo with lighter $\delta^{98/95}$Mo in soils and saprolites during chemical weathering is probably the key to these isotopic variations. Mo adsorption by suspended particulates does not change the $\delta^{98/95}$Mo of the XJR water significantly, and weathering of sulfate and sulfide minerals appears not to contribute much to the high $\delta^{98/95}$Mo values of the XJR water.
3) There is a Mo concentration and $\delta^{98/95}$Mo gradient in the water of the three largest rivers (CJR, HHR, and XJR) in China. The XJR water has the lowest Mo concentrations and heaviest $\delta^{98/95}$Mo values, whereas the HHR water has the highest Mo concentrations and lightest $\delta^{98/95}$Mo values, and those of the CJR lie between the two. The difference in the efficiency of trapping Mo in soils and saprolites, which is probably related to climatic differences among the three catchments, may account for these spatial differences in the isotopic composition of Mo. Such a mechanism apparently affects many large rivers around the world, and could be an important factor in controlling the dissolved Mo concentrations and isotopic compositions of large rivers.

Acknowledgments

The authors thank Dr. Zhang Le and Wu Lei of the State Key Laboratory of Isotope Geochemistry, GIG-CAS, for their assistance with MC-ICP-MS measurements. Thanks also go to the Editor Michael Böttcher and two anonymous reviewers for their helpful comments and constructive suggestions. This work was supported by grants from the Chinese Ministry of Science and Technology Special Scheme (Grant 2011CB808905), the GIGCAS 135 Project (Y234091001), and the National Natural Science Foundation of China (Grants 41473019 and 41325012). This is contribution IS-2091 from GIGCAS.

References

Anbar, A.D., 2004. Molybdenum stable isotopes: observations, interpretations, and directions. In: Johnson, C.M., Beard, B.L., Albarede, F. (Eds.), Geochemistry of Non-traditional Stable Isotopes, Reviews in Mineralogy and Geochemistry 55. Mineralogical Society of America, Geochemical Society, Washington, USA, pp. 429–450.
Anbar, A.D., Duan, Y., Lyons, T.W., Arnold, G.L., Kendall, B., Creaser, R.A., Kaufman, A.J., Gordon, G.W., Scott, C., Garvin, J., Buick, R., 2007. A whiff of oxygen before the Great Oxidation Event? Science 317, 1903–1906.
Archer, C., Vance, D., 2008. The isotopic signature of the global riverine molybdenum flux and anoxia in the ancient oceans. Nat. Geosci. 1 (9), 597–600.
Arnold, G., Anbar, A., Barling, J., Lyons, T., 2004. Molybdenum isotope evidence for widespread anoxia in mid-Proterozoic oceans. Science 304, 87–90.
Barling, J., Anbar, A.D., 2004. Molybdenum isotope fractionation during adsorption by manganese oxides. Earth Planet. Sci. Lett. 217 (3-4), 315–329.
Chen, Z.Y., Li, J.F., Shen, H.T., Wang, Z.H., 2001. Yangtze River of China: historical analysis of discharge variability and sediment flux. Geomorphology 41, 77–91.
Collier, R., 1985. Molybdenum in the northeast Pacific Ocean. Limnol. Oceanogr. 30 (6), 1351–1354.
Colodner, 1995. Rhenium in the Black Sea: comparison with molybdenum and uranium. Earth Planet. Sci. Lett. 131, 1–15.
Dai, S., Chou, C.L., 2007. Occurrence and origin of minerals in a chamosite-bearing coal of Late Permian age, Zhaotong, Yunnan, China. Am. Mineral. 92 (8–9), 1253–1261.
Dai, W., Huang, Y., 2006. Relation of soil organic matter concentration to climate and altitude in zonal soils of China. Catena 65 (1), 87–94.
Ding, Z.H., Zheng, B.S., Long, J.P., Belkin, H.E., Finkelman, R.B., Chen, C.G., Zhou, D.X., Zhou, Y.S., 2001. Geological and geochemical characteristics of high arsenic coals from endemic arsenosis areas in southwestern Guizhou Province, China. Appl. Geochem. 16 (11), 1353–1360.
Ding, T., Gao, J., Tian, S., Wang, H., Li, M., 2011. Silicon isotopic composition of dissolved silicon and suspended particulate matter in the Yellow River, China, with implications for the global silicon cycle. Geochim. Cosmochim. Acta 75 (21), 6672–6689.
Duan, Y., Anbar, A.D., Arnold, G.L., Lyons, T.W., Gordon, G.W., Kendall, B., 2010. Molybdenum isotope evidence for mild environmental oxygenation before the Great Oxidation Event. Geochim. Cosmochim. Acta 74 (23), 6655–6668.
Elbaz-Poulichet, F., Seyler, P., Maurice-Bourgoin, L., Guyot, J.L., Dupuy, C., 1999. Trace element geochemistry in the upper Amazon drainage basin (Bolivia). Chem. Geol. 157 (3), 319–334.
Gaillardet, J., Dupré, B., Louvat, P., Allegre, C., 1999. Global silicate weathering and CO_2 consumption rates deduced from the chemistry of large rivers. Chem. Geol. 159 (1), 3–30.
Gaillardet, J., Viers, J., Dupré, B., 2005. Trace element in river waters. In: Drever, J.L. (Ed.), Treatise on Geochemistry 5. Surface and Ground Water Weathering and Soils. Elsevier. ISBN: 0-08-043751-6, pp. 225–272.

Gao, S., Lou, T.C.M., Zhang, B.R., Zhang, H.F., Han, Y.W., Zhao, Z.D., 1999. The structure and compositions of the East China Crust. Sci. China Ser. D Earth Sci. 29 (3), 204–213.

Gao, Q.Z., Tao, Z., Huang, X.K., Nan, L., Yu, K.F., Wang, Z.G., 2009. Chemical weathering and CO_2 consumption in the Xijiang River basin, South China. Geomorphology 106 (3), 324–332.

Gill, B.C., Lyons, T.W., Young, S.A., Kump, L.R., Knoll, A.H., Saltzman, M.R., 2011. Geochemical evidence for widespread euxinia in the Later Cambrian ocean. Nature 469, 80–83.

Goldberg, T., Archer, C., Vance, D., Poulton, S., 2009. Mo isotope fractionation during adsorption to Fe (oxyhydr) oxides. Geochim. Cosmochim. Acta 73 (21), 6502–6516.

Greber, N.D., Siebert, C., Nägler, T.F., Pettke, T., 2012. $\delta^{98/95}$Mo values and molybdenum concentration data for NIST SRM 610, 612 and 3134: towards a common protocol for reporting Mo data. Geostand. Geoanal. Res. 36, 291–300.

Han, G.L., Tang, Y., Xu, Z.F., 2010. Fluvial geochemistry of rivers draining karst terrain in Southwest China. J. Asian Earth Sci. 38 (1), 65–75.

Hu, R.Z., Burnard, P.G., Turner, G., Bi, X.W., 1998. Helium and argon isotope systematics in fluid inclusions of Machangqing copper deposit in west Yunnan province, China. Chem. Geol. 146 (1), 55–63.

Huang, Z.G., Zhang, W.Q., Chen, J.H., Liu, R.H., He, Z.Z., 1996. The Red Weathering Profiles in South China. Ocean. Press, Beijing, China (in Chinese).

Kaasalainen, H., Stefánsson, A., 2012. The chemistry of trace elements in surface geothermal waters and steam, Iceland. Chem. Geol. 330, 60–85.

Kendall, B., Gordon, G.W., Poulton, S.W., Anbar, A.D., 2011. Molybdenum isotope constraints on the extent of late Paleoproterozoic ocean euxinia. Earth Planet. Sci. Lett. 307 (3–4), 450–460.

Li, X.B., Huang, Z.L., Li, W.B., Zhang, Z.L., Yan, Z.F., 2006. Sulfur isotopic compositions of the Huize super-large Pb–Zn deposit, Yunnan Province, China: implications for the source of sulfur in the ore-forming fluids. J. Geochem. Explor. 89 (1), 227–230.

Li, S.L., Calmels, D., Han, G.L., Gaillardet, J., Liu, C.Q., 2008. Sulfuric acid as an agent of carbonate weathering constrained by $\delta^{13}C_{DIC}$: examples from Southwest China. Earth Planet. Sci. Lett. 270 (3), 189–199.

Li, J., Liang, X.R., Zhong, L.F., Wang, X.C., Ren, Z.Y., Sun, S.L., Zhang, Z.F., Xu, J.F., 2014. Measurement of the isotopic composition of molybdenum in geological samples by MC-ICP-MS using a novel chromatographic extraction technique. Geostand. Geoanal. Res. 38, 345–354.

Liu, Z., Shao, M.A., Wang, Y., 2011. Effect of environmental factors on regional soil organic carbon stocks across the Loess Plateau region, China. Agric. Ecosyst. Environ. 142 (3), 184–194.

Luo, C., Zheng, H.B., Tada, R., Wu, W.H., Irino, T., Yang, S.Y., Saito, K., 2014. Tracing Sr isotopic composition in space and time across the Yangtze River basin. Chem. Geol. 388, 59–70.

Ma, J.L., Wang, Z.B., Wei, G.J., Li, J., Liu, Y., Xu, Y.G., 2015. Evidence of Mo isotope variations during extreme weathering of basalt from Hainan Island, South China. Geochim. Cosmochim. Acta (Submitted for publication).

Malinovsky, D., Rodushkin, I., Baxter, D.C., Ingri, J., Ohlander, B., 2005. Molybdenum isotope ratio measurements on geological samples by MC-ICPMS. Int. J. Mass Spectrom. 245 (1–3), 94–107.

Malinovsky, D., Hammarlund, D., Ilyashuk, B., Martinsson, O., Gelting, J., 2007. Variations in the isotopic composition of molybdenum in freshwater lake systems. Chem. Geol. 236 (3–4), 181–198.

Morford, J.L., Emerson, S., 1999. The geochemistry of redox sensitive trace metals in sediments. Geochim. Cosmochim. Acta 63 (11–12), 1735–1750.

Nägler, T.F., Anbar, A.D., Archer, C., Goldberg, T., Gordon, G.W., Greber, N.D., Siebert, C., Sohrin, Y., Vance, D., 2013. Proposal for an international molybdenum isotope measurement standard and data representation. Geostand. Geoanal. Res. 38 (2), 149–151.

Neubert, N., Heri, A., Voegelin, A.R., Nägler, T.F., Schlunegger, F., Villa, I.M., 2011. The molybdenum isotopic composition in river water: constraints from small catchments. Earth Planet. Sci. Lett. 304, 180–190.

Pearce, C.R., Cohen, A.S., Coe, A.L., Burton, K.W., 2008. Molybdenum isotope evidence for global ocean anoxia coupled with perturbations to the carbon cycle during the Early Jurassic. Geology 36 (3), 231–234.

Pearce, C.R., Cohen, A.S., Parkinson, I.J., 2009. Quantitative separation of molybdenum and rhenium from geological materials for isotopic determination by MC-ICP-MS. Geostand. Geoanal. Res. 33 (2), 219–229.

Pearce, C.R., Burton, K.W., Pogge von Strandmann, P.A.E., James, R.H., Gíslason, S., 2010a. Molybdenum isotope behaviour accompanying weathering and riverine transport in a basaltic terrain. Earth Planet. Sci. Lett. 295, 104–114.

Pearce, C.R., Coe, A.L., Cohen, A.S., 2010b. Seawater redox variations during the deposition of the Kimmeridge Clay Formation, United Kingdom (Upper Jurassic): evidence from molybdenum isotopes and trace metal ratios. Paleoceanography 25 (4), PA4213.

Pearl River Water Resources Committee, 1991. The Zhujiang Archive (in Chinese). Guangdong Sci. and Technol. vol. 1. Press Guangzhou, China.

Pett-Ridge, J., Siebert, C., Halliday, A., 2008. Molybdenum isotopes as proxy for redox conditions during weathering. Geochim. Cosmochim. Acta 72 (12), A741.

Planavsky, N.J., Asael, D., Hofmann, A., Reinhard, C.T., Lalonde, S.V., Knudsen, A., Wang, X.L., Ossa, F.O., Pecoites, E., Smith, A.J.B., Beukes, N.B., Bekker, A., Johnsn, T.M., Konhauser, K.O., Lyons, T.W., Rouxel, O.J., 2014. Evidence for oxygenic photosynthesis half a billion years before the Great Oxidation Event. Nat. Geosci. 7 (4), 283–286.

Proemse, B.C., Grasby, S.E., Wieser, M., Mayer, B., Beauchamp, B., 2013. Molybdenum isotopic evidence for oxic marine conditions during the latest Permian extinction. Geology 41 (9), 967–970.

Rahaman, W., Goswami, V., Singh, S.K., Rai, V.K., 2014. Molybdenum isotopes in two Indian estuaries: mixing characteristics and input to oceans. Geochim. Cosmochim. Acta 141, 407–422.

Shiller, A.M., 1997. Dissolved trace elements in the Mississippi River: seasonal, interannual, and decadal variability. Geochim. Cosmochim. Acta 61 (20), 4321–4330.

Siebert, C., Nägler, T.F., Kramers, J.D., 2001. Determination of molybdenum isotope fractionation by double-spike multicollector inductively coupled plasma mass spectrometry. Geochem. Geophys. Geosyst. 2, 2000GC000124.

Siebert, C., Nägler, T.F., von Blanckenburg, F., Kramers, J.D., 2003. Molybdenum isotope records as a potential new proxy for paleoceanography. Earth Planet. Sci. Lett. 211 (1–2), 159–171.

Siebert, C., Kramers, J.D., Meisel, T., Morel, P., Nägler, T.F., 2005. PGE, Re–Os, and Mo isotope systematics in Archean and early Proterozoic sedimentary systems as proxies for redox conditions of the early Earth. Geochim. Cosmochim. Acta 69 (7), 1787–1801.

Siebert, C., Burton, K., Halliday, A.N., 2009. Molybdenum isotope fractionation during continental weathering. Geochim. Cosmochim. Acta 73 (A1220-A1220).

Siebert, C., Pett-Ridge, J.C., Opfergelt, S., Guicharnaud, R.A., Halliday, A.N., Burton, K.W., 2015. Molybdenum isotope fractionation in soils: Influence of redox conditions, organic matter, and atmospheric inputs. Geochim. Cosmochim. Acta 73. http://dx.doi.org/10.1016/j.gca.2015.04.007.

Sun, H.G., Han, J.T., Li, D., Zhang, S.R., Lu, X.X., 2010. Chemical weathering inferred from riverine water chemistry in the lower Xijiang basin, South China. Sci. Total Environ. 408 (20), 4749–4760.

Voegelin, A.R., Nägler, T.F., Samankassou, E., Villa, I.M., 2009. Molybdenum isotopic composition of modern and Carboniferous carbonates. Chem. Geol. 265 (3–4), 488–498.

Voegelin, A.R., Nägler, T.F., Beukes, N.J., Lacassie, J.P., 2010. Molybdenum isotopes in late Archean carbonate rocks: implications for early Earth oxygenation. Precambrian Res. 182 (1), 70–82.

Voegelin, A.R., Nägler, T.F., Pettke, T., Neubert, N., Steinmann, M., Pourret, O., Villa, I.M., 2012. The impact of igneous bedrock weathering on the Mo isotopic composition of stream waters: natural samples and laboratory experiments. Geochim. Cosmochim. Acta 86, 150–165.

Wang, B., Lee, X.Q., Yuan, H.L., Zhou, H., Cheng, H.G., Cheng, J.Z., Zhou, Z.H., Xing, Y., Fang, B., Zhang, K.L., Yang, F., 2012. Distinct patterns of chemical weathering in the drainage basins of the Huanghe and Xijiang River, China: evidence from chemical and Sr-isotopic compositions. J. Asian Earth Sci. 59, 219–230.

Wei, G.J., Xie, L.H., Lu, W.J., Liu, Y., Deng, W.F., Zeng, T., Yang, Y.H., Sun, Y.L., 2011. Seasonal variations of the river water chemical compositions at Guiping Gaoyao and Qingyuan stations fo the Pearl River. Quat. Sci. 31 (3), 417–425 (in Chinese with English abstract).

Wei, G.J., Ma, J.L., Liu, Y., Xie, L.H., Lu, W.J., Deng, W.F., Ren, Z.Y., Zeng, T., Yang, Y.H., 2013. Seasonal changes in the radiogenic and stable strontium isotopic composition of Xijiang River water: implications for chemical weathering. Chem. Geol. 343, 67–75.

Wen, H.J., Carignan, J., Zhang, Y.X., Fan, H.F., Cloquet, C., Liu, S.R., 2011. Molybdenum isotopic records across the Precambrian–Cambrian boundary. Geology 39 (8), 775–778.

Wichard, T., Mishra, B., Myneni, S.C.B., Bellenger, J.P., Kraepiel, A.M.L., 2009. Storage and bioavailability of molybdenum in soils increased by organic matter complexation. Nat. Geosci. 2, 625–629.

Wille, M., Kramers, J., Nägler, T.F., Beukes, N., Schr der, S., Meisel, T., Lacassie, J.P., Voegelin, A.R., 2007. Evidence for a gradual rise of oxygen between 2.6 and 2.5 Ga from Mo isotopes and Re-PGE signatures in shales. Geochim. Cosmochim. Acta 71 (10), 2417–2435.

Xu, Z.F., Han, G.L., 2009. Rare earth elements (REE) of dissolved and suspended loads in the Xijiang River, South China. Appl. Geochem. 24 (9), 1803–1816.

Xu, Z.F., Liu, C.Q., 2007. Chemical weathering in the upper reaches of Xijiang River draining the Yunnan–Guizhou Plateau, Southwest China. Chem. Geol. 239 (1), 83–95.

Xu, K.H., Milliman, J.D., Xu, H., 2010. Temporal trend of precipitation and runoff in major Chinese Rivers since 1951. Glob. Planet. Chang. 73 (3), 219–232.

Xu, N., Braida, W., Christodoulatos, C., Chen, J.P., 2013a. A review of molybdenum adsorption in soils/bed sediments: speciation, mechanism, and model applications. Soil Sediment Contam. 22, 912–929.

Xu, L., Lehmann, B., Mao, J., 2013b. Seawater contribution to polymetallic Ni–Mo–PGE–Au mineralization in Early Cambrian black shales of South China: evidence from Mo isotope, PGE, trace element, and REE geochemistry. Ore Geol. Rev. 52, 66–84.

Yang, S.Y., Jung, H.S., Li, C.X., 2004. Two unique weathering regimes in the Changjiang and Huanghe drainage basins: geochemical evidence from river sediments. Sediment. Geol. 164 (1–2), 19–34.

Yang, S.Y., Li, C.X., Yokoyama, K., 2006. Elemental compositions and monazite age patterns of core sediments in the Changjiang Delta: implications for sediment provenance and development history of the Changjiang River. Earth Planet. Sci. Lett. 245, 762–776.

Yu, D.S., Shi, X.Z., Wang, H.J., Sun, W.X., Chen, J.M., Liu, Q.H., Zhao, Y.C., 2007. Regional patterns of soil organic carbon stocks in China. J. Environ. Manag. 85 (3), 680–689.

Zhang, J., Huang, W.W., Letolle, R., Jusserand, C., 1995. Major element chemistry of the Huanghe (Yellow River), China-weathering processes and chemical fluxes. J. Hydrol. 168 (1), 173–203.

Zhang, J.Y., Ren, D.Y., Zheng, C.G., Zeng, R.S., Chou, C.L., Liu, J., 2002. Trace element abundances in major minerals of Late Permian coals from southwestern Guizhou province, China. Int. J. Coal Geol. 53 (1), 55–64.

Zhang, S.R., Lu, X.X., Higgitt, D.L., Chen, C.T.A., Sun, H.G., Han, J.T., 2007. Water chemistry of the Zhujiang (Pearl River): natural processes and anthropogenic influences. J. Geophys. Res. 112, F01011. http://dx.doi.org/10.1029/2006JF000493.

Zhou, L., Shen, Y.A., Gao, S., Xie, S.C., Feng, Q.L., Su, J., Zhao, L.S., 2010. Molybdenum isotope and geochemical evidence for palaeoenvironmental change at the Ordovician–Silurian boundary, South China. Geochim. Cosmochim. Acta 74 (A1226-A1226).

Zhou, J., Du, J.Z., Moore, W.S., Qu, J.G., Zhang, G.L., 2014. Concentrations and fluxes of uranium in two major Chinese rivers: the Changjiang River and the Huanghe River. Estuar. Coast. Shelf Sci. 152, 56–64.

Zhu, L.J., Lin, J.Y., 1996. The geochemical features and evolution of laterite in the karst areas of Guizhou Province. Chin. J. Geochem. 15 (4), 353–363.